Journal of Applied Polymer Science

Aqueous, interfacial, and electrochemical polymerization pathways of aniline with thiophene: Nano size materials for supercapacitor

Umashankar Male,[1] Bal Sydulu Singu,[2] Palaniappan Srinivasan[1,3]

[1]Polymers and Functional Materials Division, CSIR—Indian Institute of Chemical Technology, Hyderabad 500 007, India

[2]Department of Chemistry, Osmania University, Hyderabad 500 007, India

[3]CSIR—Network Institutes for Solar Energy (NISE), New Delhi, India

The study is carried out at Polymers and Functional Materials Division, CSIR—Indian Institute of Chemical Technology, Hyderabad 500 007, India.

Correspondence to: P. Srinivasan (E-mail: palani74@rediffmail.com or palaniappan@iict.res.in)

ABSTRACT: Aniline was mixed with thiophene and oxidized by ammonium persulfate in the presence of sulfuric acid via an aqueous polymerization pathway (PAT-AP). Aqueous polymerization was also carried by sodium lauryl sulfate surfactant, and also by interfacial and electrochemical polymerization pathways. Polymers prepared were characterized by physical, spectral, and electrochemical methods. Nanofibers (30–60 nm diameter) was obtained in the case of aqueous polymerization pathway, whereas interfacial (40–60 nm) and electrochemical polymerization pathways show particulate (500–600 nm) morphology. Polymer samples were used as electrode materials in supercapacitor. Among the four different pathways, PAT-AP nanofibers show higher capacitance of 614 F g^{-1} at 1 mV s^{-1}. The values of specific capacitance, energy, and power densities of PAT-AP were found to be 400 F g^{-1}, 20 W h kg^{-1} and 1200 W kg^{-1}, respectively, at a current density of 2 A g^{-1}. The retention capacitance is 78% after completion of 1000 cycles. © 2015 Wiley Periodicals, Inc. J. Appl. Polym. Sci. **2015**, *132*, 42013.

KEYWORDS: applications; conducting polymers; electrochemistry; morphology

Received 28 August 2014; accepted 18 January 2015

DOI: 10.1002/app.42013

INTRODUCTION

In recent years, a research interest has focused on energy storage methods, among which supercapacitors have attracted much attention, as they can achieve a wide range of energy and power densities along with other desirable characteristics, for example, rapid charging times, high cycling stability, and temperature stability. Thus, supercapacitors can be designed to address a wide range of applications.[1–3]

supercapacitors are broadly divided into two types, electric double-layer capacitors (edlcs) and pseudocapacitors. EDLCs store energy only at the interface, so limited capacitance is achieved and suffers from low-energy density, which restricts their use alone in many fields, where high-energy density is a key requirement, whereas in case of pseudocapacitors, high capacitance is achieved because of redox reactions involving bulk of the material. Conducting polymers have shown potential applications in many areas, such as corrosion protection, radars, batteries, sensors, electrochromic cells, photovoltaic cells, etc.[4–7] Among conducting polymers, polyaniline (PANI) has received a great deal of attention due to its advantages, such as their electroactivity, low density, high electrical conductivity, environmental stability, ease of preparation, and attractive applications.

The synthesis of conducting polymers can be broadly classified into two major categories: chemical and electrochemical methods. A major advantage of chemical polymerization compared to that of electrochemical polymerization concerns the possibility of mass production at a reasonable cost. However, electrochemical polymerization gives pure polymer deposition on the electrode surface. Among the chemical polymerization methods such as conventional aqueous polymerization, surfactant-assisted soft template polymerization, and interfacial polymerization pathways, template-assisted polymerization is known to control the morphology of the samples, and in addition, it results in the formation of polyaniline salt containing dual dopants (acid dopant and long-chain surfactant group) with higher yield and conductivity. Interfacial polymerization is a slow process that in turn limits the secondary growth of the polymer.

Although conducting polymer-based supercapacitors have many desired properties, still it requires extensive modifications to reach the commercial market. Considerable attention has, therefore, been paid to the synthesis of various types of composite

and copolymer materials. It was revealed that, compared with homopolymers, the copolymers have higher stability and lower conductivity.[8] One of the primary purposes of the present work is to synthesize a copolymer that combines the useful properties of homopolymers. Only very few reports are available in the synthesis of copolymer of aniline with thiophene monomer. Copolymerization of aniline with thiophene is generally being carried out by electrochemical polymerization method. Bithiophene was used for copolymerization instead of thiophene;[9] however, thiophene is more conventional. Talu *et al.* could synthesize aniline and thiophene copolymers and composites in acidic ($HClO_4$) medium on platinum electrode.[10] Can *et al.* also used acidified medium (HBF_4) and obtained aniline/thiophene copolymer on platinum electrode.[11]

In the present paper, polymerization of aniline and thiophene is carried out in aqueous 1 *M* H_2SO_4 by electrochemical and chemical methods viz., aqueous and interfacial polymerization pathways. The synthesized polymers were used as electrode materials in symmetric supercapacitor in aqueous 1 *M* H_2SO_4 electrolyte. The performance of supercapacitor is evaluated by cyclic voltammetry (CV), galvanostatic charge/discharge (CD), and electrochemical impedance spectroscopy (EIS) measurements. The capacitive properties, physical, electrical, and spectral characteristics are also compared.

EXPERIMENTAL

Aniline (S. D. Fine Chemicals, India) was distilled under reduced pressure. Ammonium persulfate (APS), sodium lauryl sulfate (SLS), sulfuric acid (H_2SO_4) (Rankem, India), and thiophene (Sigma-Aldrich) were used as received. All the reactions were carried out with distilled water and solvents were distilled and used.

Aqueous Polymerization

Monomer solution was prepared by dissolving aniline (0.09 *M*) and thiophene (0.03 *M*) in 50 mL of 1 *M* H_2SO_4. The oxidant solution was prepared by dissolving ammonium persulfate (0.12 *M*) in 50 mL of 1 *M* H_2SO_4. The oxidant solution was mixed with a monomer solution at ambient atmosphere and stirred for 24 h. Then, the reaction mixture was filtered, and the residue was washed with an excess of distilled water and acetone to remove the unreacted component and oligomers. The resulting powder was dried in an oven at 50°C till a constant weight.

For comparison, polyaniline was synthesized by following the above procedure without use of thiophene and is designated as PANI in this work.

Aqueous Polymerization in the Presence of Sodium Lauryl Sulfate

Polymerization was carried out by the above aqueous polymerization procedure by dissolving sodium lauryl sulfate (0.012 *M*) along with monomers in the monomer solution.

Interfacial Polymerization

Aniline (0.09 *M*) and thiophene (0.03 *M*) were dissolved in 50 mL of chloroform, which is designated as the organic phase. The oxidant solution was prepared by dissolving ammonium persulfate (0.12 *M*) in 50 mL of 1 *M* H_2SO_4, that is, aqueous phase. Then, the two solutions were transferred into a beaker, generating an interface between the organic phase and the aqueous phase. Polymerization was carried out at the interface under static conditions for 24 h and ambient conditions. Then, reaction mixture was filtered, and the residue was washed with an excess of distilled water and acetone to remove the unreacted component and oligomers. the resulting powder was dried in an oven at 50°C till a constant weight.

Electrochemical Polymerization

Electrochemical polymerization was performed in a one compartment cell using a platinum foil as the counter electrode, a saturated calomel electrode (SCE) as the reference electrode, and a stainless steel foil as a working electrode. All potentials were relative to the SCE. The electrolyte solution for electrochemical polymerization consisted of aniline (0.09 *M*) and thiophene (0.03 *M*) in 100 mL of 1 *M* H_2SO_4 solution. The deposition of polymer was carried out by the potentiodynamic method in the voltage range of −0.2 to 0.8 V with a scan rate of 50 mV s^{-1} for 200 cycles. The obtained cyclic voltammogram shows peaks similar to that of the reported polyaniline.[12] The obtained polymer is coated on stainless steel in powder form.

CHARACTERIZATION

Polymer samples were pressed into disks of 13 mm in diameter and about 1.5 mm in thickness under a pressure of 120 kg cm^{-2}. The resistances of the pressed pellets were measured by a four probe method using a constant current source (6220) and nanovoltmeter (2182 A) (Keithley, Cleveland, Ohio). Polymer samples for Fourier transform infrared spectroscopy (FTIR) analysis was mixed with KBr powder and compressed into pellets, wherein the sample powder was evenly dispersed in KBr. FTIR spectra were recorded with a gas chromatography–FTIR spectrometer (model 670, Nicolet Nexus, Minnesota). X-ray diffractogram profiles for the powders were obtained on a Bruker AXS D8 advance X-ray diffractometer (Karlsruhe, Germany) with Cu K_α ($\lambda = 1.54$ Å) radiation (land continuous) at a scan speed of 0.045 min^{-1}. Powder samples were used by employing a standard sample holder. The *d*-spacing was calculated from the angular position 2θ of the observed reflection peaks based on the bragg's formula ($2d\sin\theta = n\lambda$), where λ is the wavelength of X-ray beam and θ is the diffraction angle. Morphology studies of the polymer powder samples were carried out with Hitachi S-4300 SE/N field emission scanning electron microscope (FESEM) (Hitachi, Tokyo, Japan) operating at 20 kV. The powder sample was sputtered on a carbon disc with the help of double-sided adhesive tape. Transmission electron microscopy (TEM) measurement was carried out with Hitachi S-5500 instrument operated at an accelerate voltage of 30 kV. The sample was prepared by casting sample dispersion on carbon-coated copper grids (300 mesh) and allowed to dry at room temperature. Thermo gravimetric analysis (TGA) was performed with a TGA Q500 Universal (TA Instruments, UK) at a heating rate of 10°C min^{-1} under nitrogen atmosphere.

Electrochemical Analysis

The working electrodes were prepared by pressing the polymeric sample (5 mg) on stainless steel mesh (316 grade) by the

application of 120 kg cm^{-2} of pressure without any additional binder. The electrochemical performances of all the polymer samples were investigated using two-electrode system cells without a reference electrode. Two electrodes with identical sample were separated by cotton cloth and assembled as supercapacitor. Cyclic voltammetry and galvanostatic charge/discharge experiments were performed with a WMPG1000 multichannel potentiostat/galvanostat (WonATech, Gyeonggi-do, Korea). Cyclic voltammograms (CV) were recorded from −0.2 to 0.6 V at various sweep rates and charge/discharge experiments were carried out from 0.0 to 0.6 V at various current densities. Electrochemical impedance spectroscopy measurements were carried out with IM6ex (zahner-Elektrik, Germany) by applying an AC voltage of 5 mV amplitude in the 40 kHz to 10 mHz frequency range, at 0.6 and 0.8 V using three electrode cell configuration, that is, polymer electrode as a working electrode, platinum foil as a counter electrode, and calomel electrode as a reference electrode. All electrochemical measurements were carried out at ambient temperature and 1 *M* H_2SO_4 was used as the electrolyte solution.

RESULTS AND DISCUSSION

In this work, aniline was chemically oxidized in the presence of thiophene in sulfuric acid by ammonium persulfate via aqueous (with and without the use of soft template) and interfacial polymerization pathways. Also, aniline was electrochemically oxidized in the presence of thiophene in sulfuric acid by potentiodynamic method. The properties of these materials are discussed here in comparison with the homopolymer of polyaniline salt prepared by chemical oxidation pathway. However, polymerization of thiophene did not proceed in the chemical oxidation pathway.

FTIR Studies

Figure 1 represents the fourier transform infrared spectra of polymers synthesized by aqueous, aqueous-SLS, interfacial, and electrochemical polymerization methods along with pure polyaniline salt for comparison. The careful examination of all the spectra [Figure 1(a–d)] reveals that all the polymer samples have all the characteristic peaks of pure polyaniline salt [Figure 1(e)], that is, at 3420 cm^{-1} (N—H stretching), 1565 cm^{-1} (C=C stretching, quinonoid ring), 1480 cm^{-1} (C=C stretching, benzenoid ring), 1295 cm^{-1} (C—N stretching, quinonoid ring), 1245 cm^{-1} (C=N stretching, benzenoid ring), 1105 cm^{-1} (electronic vibrational band), and 800 cm^{-1} (1,4-disubstituted benzene). In addition, a peak at ~750 cm^{-1} was observed due to C—S bending,[13] which indicates the presence of thiophene unit in the polymer chain. In the case of FTIR spectrum of PAT-AP-SLS, that is, the use of SLS in the polymerization reaction, show peaks at 2925, 2850, 1650, and 1750 cm^{-1} in addition to the normal peaks of polyaniline. The sharp and intense peaks at 2925 and 2850 cm^{-1} are due to C—H stretching vibration of SLS[14] and a peak at 1650 cm^{-1} is due to the stretching of sulfonate (S=O) group of SLS. This result indicates that the SLS is doped onto the polymer chain in the form of dodecylhydrogen sulfate (DHS) in PAT-AP-SLS. A peak at 1750 cm^{-1} is due to over oxidation and this result signpost that the use of SLS leads to over oxidation of aniline to polyaniline salt.

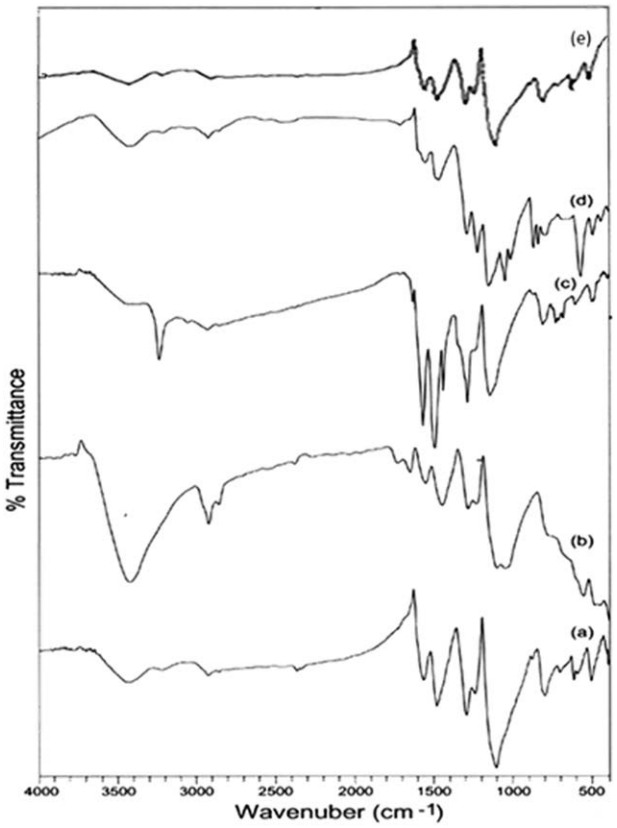

Figure 1. FTIR spectra of (a) PAT-AP, (b) PAT-AP –SLS, (c) PAT-IP, (d) PAT-EP, and (e) PANI.

X-ray Diffraction Studies

X-ray diffractograms of polymer samples prepared by four different pathways along with pure polyaniline salt are shown in Figure 2. PAT-AP [Figure 2(a)] prepared by aqueous polymerization pathway shows peaks at 2θ values of 20°, 25°, and 27° corresponding to *d*-spacings of 3.5, 3.3, and 1.7 Å, respectively, and are similar to the X-ray diffraction pattern of polyaniline salt [Figure 2(e)].[15] The X-ray diffraction pattern of PAT-AP-SLS [Figure 2(b)] prepared using SLS shows similar peaks of PAT-AP with an additional sharp, intense peak at 2θ value of 6.5° corresponding to a *d*-spacing of 13.5 Å, this peak is generally observed due to the presence of long aliphatic chain. This result indicates the presence of dodecyl hydrogen sulfate (DHS) in PAT-AP-SLS. Moreover, PAT-AP-SLS shows higher crystallinity when compared to that of PAT-AP. This degree of crystallinity can be ascribed to increasing the content of PANI in the obtained composites. Thus, increasing the amount of PANI might be accompanied by increasing the molecular weight of the PANI and the amount of doping anions (H_2SO_4 and DHS).[16] X-ray diffraction pattern of sample prepared by interfacial polymerization pathway (PAT-IP) shows less crystallinity than that of PAT-AP with peaks at 2θ values of 8.7°, 14.5°, 20.5°, and 25.5° corresponding to *d*-spacings of 12.2, 10.1, 4.3, and 3.5 Å, respectively [Figure 2(c)]. The crystalline nature is further decreased in the case of PAT-EP (Figure 2d) with peaks at 2θ values of 12°, 20°, and 25° corresponding *d*-spacings are 7.3, 4.4, and 3.5 Å, respectively. X-ray diffractogram of

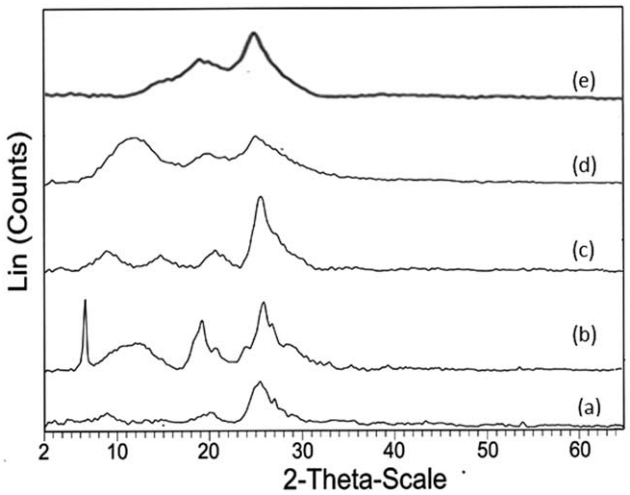

Figure 2. XRD patterns of (a) PAT-AP, (b) PAT-AP –SLS, (c) PAT-IP, (d) PAT-EP, and (e) PANI.

polymeric materials synthesized via different polymerization pathways show different orders of crystallinity.

Morphology Studies

Morphological properties of the polymer samples prepared by four different pathways along with pure polyaniline salt were found out using FESEM and are shown in Figure 3. Nano fiber morphology was observed for pure polyaniline salt [Figure 3(a)]. When thiophene is used in the polymerization reaction, the nano fiber morphology of polyaniline salt is slightly changed with diameters of ~30–60 nm [Figure 3(b)], and with the use of SLS in the reaction, the diameter of polymers decreased to ~ 20–50 nm [Figure 3(c)]. Fewer diameters with the use of SLS might be expected because of enough nucleation sites available for monomer before oxidation begins, whereas in the absence of SLS, agglomeration of the polymer takes place which results in nanofibers with higher diameter. However, PAT sample prepared by interfacial polymerization pathway shows nano particle

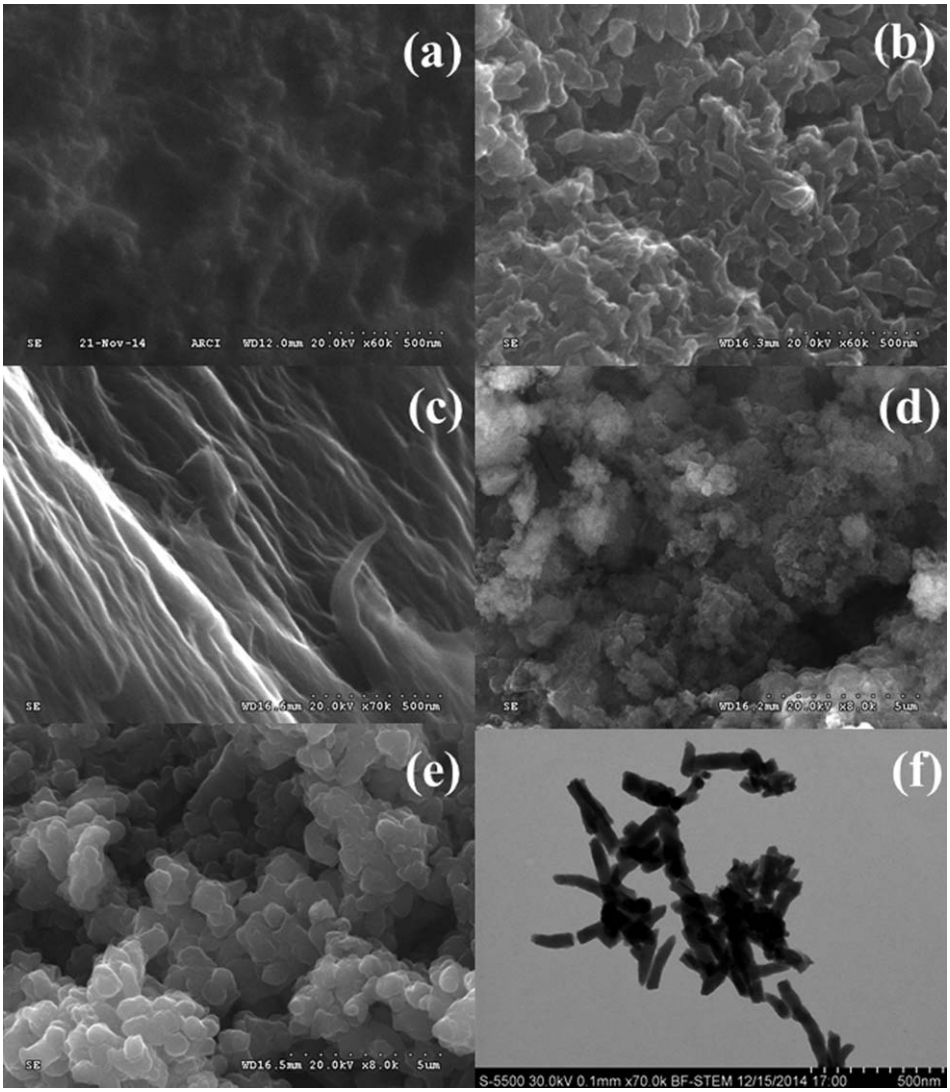

Figure 3. FESEM pictures of (a) PANI, (b) PAT-AP, (c) PAT-AP-SLS, (d) PAT-IP, (e) PAT-EP, and (f) TEM picture of PAT-AP-SLS.

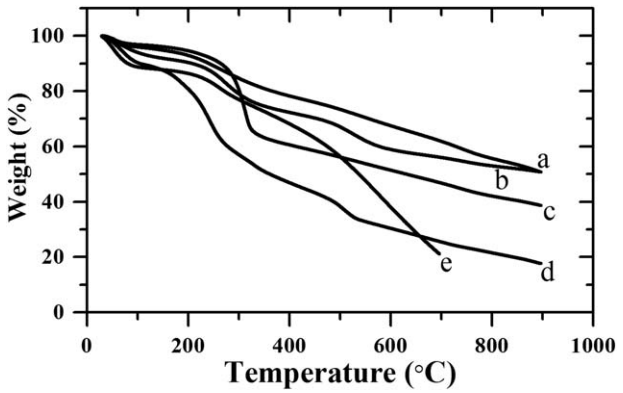

Figure 4. Thermograms of (a) PAT-AP, (b) PAT-AP –SLS, (c) PAT-IP, (d) PAT-EP, and (e) PANI.

morphology with 40–60 nm size [Figure 3(d)] and the PAT sample prepared by electrochemical polymerization pathway also shows sphere like morphology with diameter of 500–600 nm [Figure 3(e)]. In order to clearly find out the morphologoy of PAT-AP-SLS, TEM for PAT-AP-SLS sample was recorded [Figure 3(f)] and it supports the nano fibrous morphology as observed from FESEM analysis [Figure 3(c)].

Thermal Analysis

Thermal behaviors of polymer samples were analyzed by thermal gravimetric analysis (TGA) under nitrogen atmosphere, and the thermograms were shown in Figure 4. The thermal degradation of polymers shows a three-step weight loss process, as can be seen in Figure 4. The first weight loss at approximately 110°C is attributed to the loss of water molecules/moisture present in the polymer and the weight loss from 190 to 230°C results from the elimination of dopant anions from the polymer matrix. In fact, a considerable amount of water content is essential for an electrode material as it is conducive for ionic transportation in an electrolyte, thus enhancing electrochemical performance.[17,18] PAT-AP sample is stable up to 190°C, and the stability increases with the use of sodium lauryl sulfate (210°C), this is due to the increasing the molecular weight of the PANI and the amount of doping anions (H_2SO_4 and DHS). However, the stability of the sample is higher in the case of the sample prepared by interfacial polymerization pathway (230°C). Stability of a sample prepared by electrochemical polymerization pathway (180°C) is less compared to other samples. The third weight loss, from approximately 400 to 600°C, corresponds to the thermal decomposition of the PANI.

Yield and Conductivity Studies

Yield and conductivities of the polymers synthesized in this work are reported in Table I. Yield is reported in grams because the composition of the polymer cannot be determined from the present study. The yield of polymer samples prepared by aqueous polymerization pathway (PAT-AP) is 1.6 *g* (yield with respect to the amount of aniline—1.75 *g*; thiophene—0.5 *g*) and the yield increased to 1.9 *g* with the use of SLS in the reaction. This result indicates that SLS increases the doping efficiency of aniline by doping dodecyl hydrogen sulfate (DHS) onto the polymer.[19] The doping of DHS in the polymer sample is also supported by FTIR and XRD. However, the value of conductivity remains same for

Table I. Yield and Conductivity Values of PANI and PAT Samples

Method	Yield (*g*)	Conductivity (S cm^{-1})
PAT-AP	1.6	0.4
PAT-AP-SLS	1.9	0.4
PAT-IP	0.8	0.02
PAT-EP[a]	-	-
PANI	1.5	1.3

[a] Less amount of powder was formed on the electrode surface, and hence, pellet could not be made to measure the conductivity.

both PAT–AP and PAT-AP-SLS (0.4 S cm^{-1}). This result suggests that the addition of anionic surfactant SLS, does not show much effect on the conductivity value. The yield in the case of interfacial polymerization (PAT-IP) is less, that is, 0.8 *g* as expected because polymerization occurs only at the interface, which is not that much effective when compared to that of aqueous polymerization pathway, wherein continuous mixing take place among the reactants. Conductivity value of PAT-IP is 0.02 S cm^{-1}. Yield of the pure polyaniline-sulfate salt is found to be almost the same with that of PAT-AP. However, conductivity (1.3 S cm^{-1}) is found to be higher than that of PAT-AP (0.4 S cm^{-1}). This result indicates that the conjugation of polyaniline is affected by the addition of thiophene units.

Cyclic Voltammetry

Symmetric cells of polymer samples synthesized by four different polymerization pathways were subjected to cyclic voltammetry measurements. As a representative system, the cyclic voltammograms (CV) of PAT-AP at different scan rates is shown in Figure 5. Voltammograms are almost rectangular with good symmetry, showing a good capacitive behavior of the electrode materials. A similar quasi-rectangular shape was maintained as the scan rate was increased to 10 mV s^{-1}, proving the fast access of ions to the surface of the nanofibers. The specific capacitance C_s was calculated from CV using the following formula.[20]

$$C_s = \frac{2 \cdot i}{v \cdot m} \quad (1)$$

Where, C_s is specific capacitance, i is the average current from anodic and cathodic curves, v is the scan rate, and m is the mass of one electrode. The specific capacitance of PAT-AP, PAT-AP-SLS, PAT-IP, and PAT-EP as a function of scan rate is shown

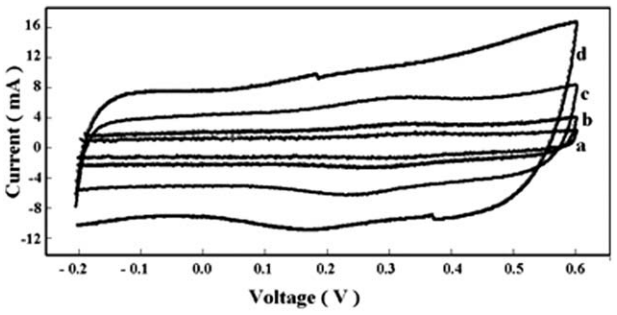

Figure 5. Cyclic voltammograms of PAT-AP symmetric cell at different sweep rates (a) 1, (b) 2, (c) 5, and (d) 10 mV s^{-1}.

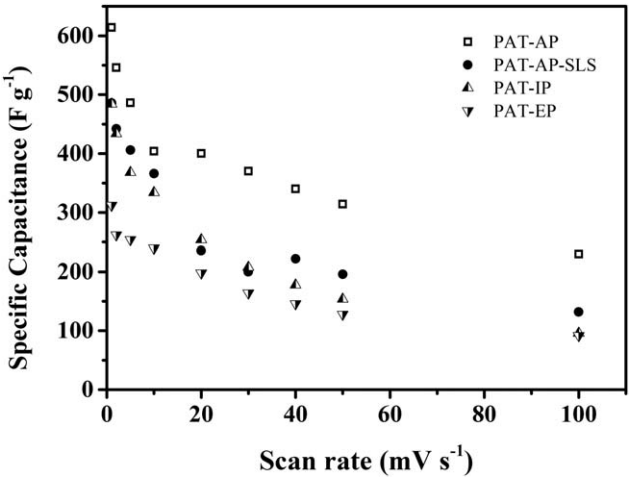

Figure 6. Specific capacitance of (a) PAT-AP, (b) PAT-AP-SLS, (c) PAT-IP, and (d) PAT-EP as a function of scan rate.

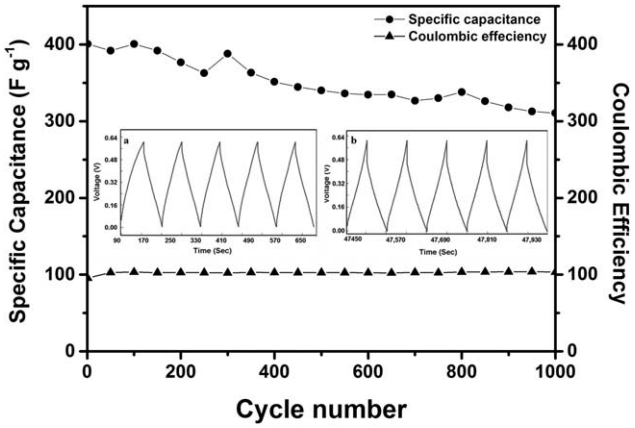

Figure 7. Specific capacitance and columbic efficiency as a function of cycle number for PAT-AP at 2 A g^{-1} current density. (Inset: galvanostatic charge–discharge curves of PAT-AP symmetric cell at 2 A g^{-1} current density (a) 1st to 5th cycles and (b) 996th to 1000th cycles.)

in Figure 6. At different scan rates, in the reduction part, a small shift to negative direction of potential is obtained due to uneven current distribution vis-a-vis partial double-layer charging. From the figure, it can be observed that the capacitance value decreases with increasing scan rate, and it can be because of two reasons: (i) as the scan rate increases, the electric charge might have the difficulty to occupy all the available sites at electrode/electrolyte interface due to their limited range of migration and orientation in the electrolyte and (ii) due to internal resistance of the supercapacitor.[21] Among the four different pathways, PAT-AP nanofibers shows higher specific capacitance (614 F g^{-1} at 1 mV s^{-1}) throughout all scan rates compared to that of the other polymerization pathways, that is, PAT-AP-SLS (486 F g^{-1}), PAT-IP (484 F g^{-1}), and PAT-EP (312 F g^{-1}). Interfacial polymerization is a slow process that results in lower yield and conductivity compared to that of the sample prepared by aqueous polymerization pathway. Lower capacitance value of PAT-IP is due to its lower conductivity. Use of SLS surfactant in PAT-AP-SLS results in the formation of polyaniline salt containing sulfate and dodecylhydrogen sulfate dopants. The presence of long-chain surfactant group reduces the movement of ions to the electrode surface which in turn results in lower capacitance.

Since the PAT-AP sample showed higher specific capacitance value from cyclic voltammetry studies, further studies are carried for PAT-AP sample, that is, charge/discharge (cycle life) and electrochemical impedance measurements.

Cycle Life

Cycle life is an important parameter for supercapacitor applications. Cyclic stability of PAT-AP electrode was evaluated by galvanostatic charge/discharge (CD) behavior. CD measurement was carried out at 2 A g^{-1} current density within the potential window of 0.0 to 0.6 V for 1000 continuous cycles and the charge–discharge curves were shown as an inset in Figure 7.

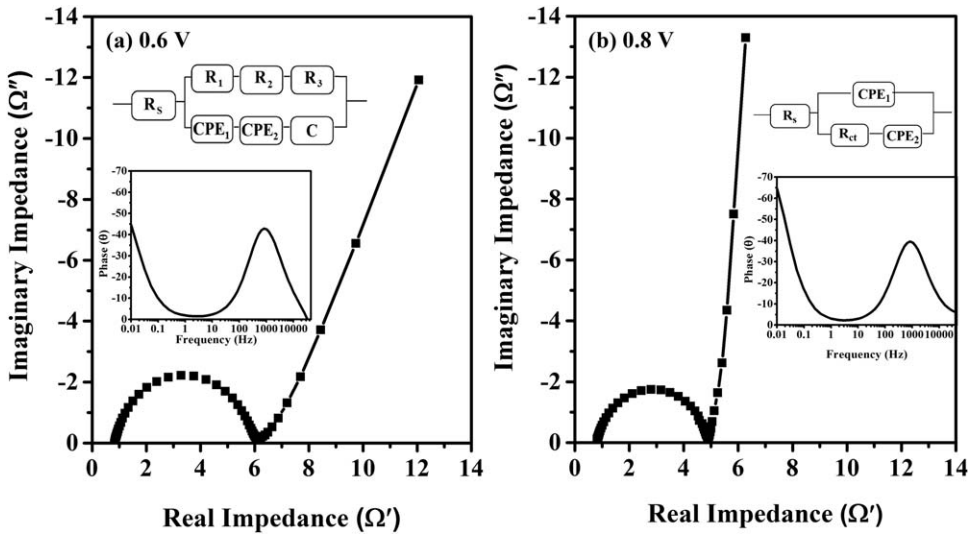

Figure 8. Nyquist plots of PAT-AP in the frequency range of 40 kHz to 10 mHz at (a) 0.6 V and (c) 0.8 V. (Inset: corresponding bode plots and circuit diagrams)

The almost triangular shape of the curves reveals a fast and reversible faradic reaction for charge storage.

The value of specific capacitance is calculated using the formula $C_d = (2 \cdot i \cdot \Delta t)/(\Delta v \cdot m)$ where C_d is the specific capacitance from charge discharge, i is the current density, Δt is the discharge time, Δv is the voltage drop during the period of discharge, and m is the mass of material in one electrode.[22,23] Figure 7 represents the specific capacitance and columbic efficiency as a function of cycle number. The specific capacitance value decreases from 400 to 310 F g^{-1} for the 1st and 1000th cycles, respectively, at 2 A g^{-1}. The decrease in capacitance value with the number of cycles is due to doping and dedoping of H^+ into or from the polymer chains during charge and discharge cycles, which results in swelling and shrinkage of polymeric material. However, columbic efficiency is almost remains constant (100–98%) up to 1000 cycles. The energy and power densities at 2 A g^{-1} is found to be 20 W h kg^{-1}, and 1200 W kg^{-1}, respectively.

Electrochemical Impedance Spectroscopy

Generally, polyaniline exhibits good behavior between the applied voltages of 0.6 and 0.8 V. Hence, EIS measurements were carried out for PAT-AP electrode in the frequency range from 40 kHz–10 mHz at two different voltages of 0.6 and 0.8 V and the corresponding nyquist and bode plots are shown in Figure 8. A single depressed semicircle in the high-frequency region and a straight line in the low-frequency region were observed. The high-frequency intercept on the real axis gives the solution resistance (R_s) of the materials, and the diameter of the semicircle provides the charge transfer resistance (R_{ct}). R_s values of the PAT-AP sample carried out at 0.6 and 0.8 V is same (0.8 Ω). R_{ct} value decreased as 5.3 to 4.1 Ω as applied voltage increased, that is, from 0.6 to 0.8 V. Double-layer capacitance (C_{dl}) was calculated from the semicircle and are found to be 0.15 and 0.17 mF, respectively. Time constant (τ) was calculated from the maximum of the semicircle and found to be 0.48 ms at both 0.6 and 0.8 V. Lower time constant is the property of fast charge-discharge process.[12,24] The tilted straight line at low frequencies has long been known for electrodes with inhomogeneity, porosity and/or other nonidealities.[25,26] The specific capacitance was calculated in the low-frequency region at 10 mHz and found to be 267 and 240 F g^{-1} at 0.6 and 0.8 V, respectively.

The phase angle of the PAT-AP system was obtained from the bode plot, the phase angle (Φ) of an ideal capacitor is "−90°." The phase angle obtained when the applied potential of 0.6 and 0.8 V are −45° and −65°, respectively (Figure 8).

Equivalent circuit was obtained directly from the instrument after the simulation of experimental data using Zman software supplied with the electrochemical workstation and shown as an inset in Figure 8. The circuit consists of bulk solution resistance (R_s), charge transfer resistance (R_{ct}), constant phase elements (CPE_1 and CPE_2) resistors (R_1, R_2, and R_3) and capacitor (C).

CONCLUSIONS

Polyaniline was synthesized via aqueous, interfacial, and electrochemical polymerization pathways in the presence of thiophene. Nanofiber was obtained in the case of aqueous polymerization pathway, whereas interfacial and electrochemical polymerization pathways showed sphere like particle morphology. Different crystallinity was observed for different polymerization pathways. Polymer samples were used as electrode materials in supercapacitor performance. Among the different polymerization pathways polymer sample synthesized by aqueous polymerization pathway shows better supercapacitor performance. PAT-AP shows a specific capacitance of 400 F g^{-1} with energy density of 20 W h kg^{-1} and 1200 W kg^{-1} power density. Even after completion of 1000 cycles 78% of capacitance was retained with a columbic efficiency of 99–100%.

ACKNOWLEDGEMENT

The authors thank CSIR, New Delhi under the TAPSUN program (NWP-0056) for funding. We are thankful to Dr. M. Lakshmi Kantam, Director, and Dr. K.V.S.N. Raju, CSIR-IICT for their support and encouragement. We also thank Dr. Vijayamohanan K Pillai, Director, and Dr. S. Gopukumar, CSIR-CECRI for his valuable discussion. UM is thankful to CSIR, India, and SBS is thankful to UGC, India for financial assistance.

REFERENCES

1. Snook, G. A.; Kao, P.; Best, A. S. *J. Power Sources* **2011**, *196*, 1.
2. Wang, G. P.; Zhang, L.; Zhang, J. *J. Chem. Soc. Rev.* **2012**, *41*, 797.
3. Zhao, X.; Sanchez, B. M.; Dobson, P. J.; Grant, P. S. *Nanoscale* **2011**, *3*, 839.
4. Wang, Y.; Tran, H.; Kaner, R. *Macromol. Rapid. Commun.* **2011**, *32*, 35.
5. Beaujuge, P.; Amb, C.; Reynolds, J. *Acc. Chem. Res.* **2010**, *43*, 1396.
6. Pecher, J.; Mecking, S. *Chem. Rev.* **2010**, *110*, 6260.
7. Park, D.; Kim, M.; Joo, J. *Chem. Soc. Rev.* **2010**, *39*, 2439.
8. Dimitriev, O. P.; Ogurtsov, N. A.; Pud, A. A.; Smertenko, P. S.; Piryatinski, Y. P.; Noskov,Y. V.; Kutsenko, A. S.; Shapoval, G. S. *J. Phys. Chem. C* **2008**, *112*, 14745.
9. Hu, X.; Wang, G.; Ng, H.; Wong, T. *Chem. Lett.* **1999**, *12*, 1323.
10. Talu, M.; Kabasakaloglu, M.; Oskoui, H. *J. Polym. Sci., Part A: Polym. Chem.* **1996**, *34*, 2981.
11. Can, M.; Pekmez, K.; Pekmez, N.; Yildiz, A. *Synth. Met.* **1999**, *104*, 9.
12. Girija, T. C.; Sangaranarayanan, M. V. *J. Power Sources* **2006**, *156*, 705.
13. Gnanakan, S. R. P.; Rajasekhar, M.; Subramania, A. *Int. J. Electrochem. Sci.* **2009**, *4*, 1289.
14. Singu, B. S.; Srinivasan, P.; Pabba, S. J. *Electrochem. Soc.* **2012**, *159*, A6.
15. Singu, B.; Male, U.; Srinivasan, P.; Pabba, S. J. *Solid State Electrochem.* **2014**, *18*, 1995.

16. Gemeay, A. H.; El-Sharkawy, R. G.; Mansour, I. A.; Zaki, A. B. *J. Colloid Interface Sci.* **2007**, *308*, 385.
17. Ragupathy, P.; Park, D. H.; Campet, G.; Vasan, H. N.; Hwang, S. J.; Choy, J. H.; Munichandraiah, N. *J. Phys. Chem. C* **2009**, *113*, 6303.
18. Wang, Y. T.; Lu, A. H.; Zhang, H. L.; Li, W. C. *J. Phys. Chem. C* **2011**, *115*, 5413.
19. Stejskal, J.; Omastova, M.; Fedorova, S.; Prokes, J.; Trchova, M. *Polymer* **2003**, *44*, 1353.
20. Chen, J.; Jia, C.; Wan, Z. *Electrochim. Acta* **2014**, *121*, 49.
21. Sivaraman, P.; Rath, S. K.; Hande, V. R.; Thakur, A. P.; Patri, M.; Samui, A. B. *Synth. Met.* **2006**, *156*, 1057.
22. Wang, X.; Wang, X.; Liu, L.; Yi, L.; Hu, C.; Zhang, X.; Yi, W. *Synth. Met.* **2011**, *161*, 1725.
23. Uppugalla, S.; Male, U.; Srinivasan, P. *Electrochim. Acta* **2014**, *146*, 242.
24. Burke, A. *J. Power Sources* **2000**, *91*, 37.
25. Arnott, J. B.; Browning, G. J.; Donne, S. W. *J. Electrochem. Soc.* **2006**, *153*, A1332.
26. Kerner, Z.; Pajkossy, T. *Electrochim. Acta* **2000**, *46*, 207.